

Pressure-induced structural instability of cesium halides from *ab initio* pseudopotential techniques

Stefano Baroni

*Dipartimento di Fisica Teorica, Università degli Studi di Trieste, I-34014 Trieste-Grignano, Italy
and Gruppo Nazionale di Struttura della Materia, Consiglio Nazionale delle Ricerche, I-34014 Trieste, Italy*

Paolo Giannozzi

Institut de Physique Théorique, Université de Lausanne, CH-1015 Lausanne-Dorigny, Switzerland

(Received 21 July 1986)

The structural stability of the cubic phase of CsI versus tetragonal distortions is studied from first principles using state-of-the-art local-density techniques, namely, norm-conserving pseudopotentials and large plane-wave basis sets. The effects of the polarization of the cation are explicitly accounted for using a pseudopotential that sustains the Cs $5s$ and $5p$ bands. We find that, in agreement with recent x-ray diffraction experiments and with previous theoretical work, the tetragonal phase is more stable at volumes smaller than 0.54 of the zero-pressure value. The mechanism of transition is revealed in terms of the balance between the Madelung and repulsive interionic interactions. We find that at volumes smaller than the transition volume the cubic phase is metastable, thus indicating that the transition is first order. The electron-charge-density rearrangements following compression and distortion are also examined. No evidence of a further transition to an even lower-symmetry structure has been found in a preliminary search.

I. INTRODUCTION

In recent years, the diamond-anvil-cell technology has opened a major breakthrough in the physics of materials at very high pressures. Among the unsuspected features of the high-pressure behavior of solids, one of the most spectacular is the spontaneous lowering of the symmetry of some cubic compounds.^{1,2}

As a specific example, we consider in this paper the case of CsI which undergoes a transition from the cubic to the tetragonal structure at a pressure of ~ 400 kbar.¹ At this transition, which is isovolumic within the experimental uncertainties, the volume of the unit cell is reduced to 0.54 of the zero-pressure value.

Some theoretical investigations of the high-pressure structural properties of CsI already exist: The mechanism of transition was first explained in terms of the competition between the electrostatic and repulsive interionic interactions in a simple Born-Mayer model;³ this model, although correctly displaying the mechanism of transition, suffers the disadvantage of being semiempirical: in fact the parameters of the model which reproduce the high-pressure behavior of CsI are such that the zero-pressure structure of this compound is incorrectly predicted to be rocksalt.⁴ An *ab initio* description of the high-pressure phases of CsI was then given in the framework of the atomic-spheres-approximation linear-muffin-tin-orbitals (ASA-LMTO) method.⁵ In this work, however, the deviations of the crystal charge density from the superposition of spherical muffin-tin ionic distributions were treated in an approximate way.

In this paper the high-pressure structural properties of CsI are studied from first principles without any simplifying assumption on the shape of the electron charge distri-

bution. To this aim, the electronic structure of the crystal is worked out using norm-conserving pseudopotentials and large plane-wave basis sets.

The practical equivalence of first-principles calculations based on either pseudopotential or all-electron techniques has been recently demonstrated for covalently bonded materials at volumes close to their zero-pressure values.⁶ Our results show that the above equivalence still holds in such an extreme situation of ionic compounds squeezed at $\frac{1}{2}$ of their zero-pressure volume.

II. METHOD

Total energies of CsI at various volumes and for different crystal structures have been calculated self-consistently within the local-density approximation (LDA) using nonlocal norm-conserving pseudopotentials⁷ and large plane-wave basis sets. The electron-gas exchange-correlation energy and potential used here are those determined by Ceperley and Alder⁸ as interpolated by Perdew and Zunger.⁹ We have assumed the following form for the nonlocal ionic pseudopotentials:

$$V_{\text{ion}}(\mathbf{r}, \mathbf{r}') = \frac{1}{r^2} \sum_l P_l(\hat{\mathbf{r}}, \hat{\mathbf{r}}') \delta(r - r') v_l(r), \quad (1)$$

where the P_l 's are projectors over the l angular momentum states, and the v_l 's have been determined using the Kerker's procedure.¹⁰ Angular momenta up to $l=3$ have been included and the f potential has been considered as the local reference one.

Electrons up to and including Cs $4d$ and I $4d$ have been considered as core electrons. The inclusion of the Cs $5s$ and $5p$ states into the valence shell is needed in order to obtain sensible results. In fact we found that pseudopo-

tentials which sustain only the Cs 6s electron as a valence electron (both those generated by the Kerker's scheme and those tabulated in Ref. 11) yield a monotonic lowering of the energy at decreasing volume, with no stability at all. The stability of alkali halides is due to the orthogonalization-induced repulsion between neighboring anionic and cationic orbitals. In most applications of the pseudopotential technique to semiconducting and metallic materials, the repulsion exerted by the ionic pseudopotential mainly acts on orbitals centered around the ion itself which are therefore atomic-like. It is not surprising that the simulation of the orthogonality effects between off-center orbitals by a simple atomic potential is a much more difficult task. Rather than looking for a cure of the above pathology, we have preferred to include the Cs 5s and 5p orbitals into the core for the following reasons. First of all, the orthogonality between relevant neighboring orbitals is accounted for exactly in this way. Secondly, the effects due to the relaxation of the cationic core are taken into account as well: These are not negligible in such a large-core atom as Cs. Last but not least, the inclusion of Cs 5s and 5p orbitals in the valence shell does not affect significantly the numerical labor of the computation since the spatial extension of these orbitals is comparable to that of the iodine 5s and 5p orbitals. The plane-wave basis set necessary to describe the latter is thus also adequate for the former.

The v_l 's so obtained have then been least-squares fitted to the following functional form:

$$v_l(r) = \frac{-Z_v}{r} \operatorname{erf}(r\sqrt{\alpha_c}) + \sum_{n=1}^3 (a_n + b_n r^2) e^{-\alpha_n r^2}. \quad (2)$$

Atomic Rydberg units are used throughout. The relevant parameters are summarized in Table I. The self-consistent electron density is evaluated using the (12,12,12) Monkhorst-Pack mesh¹² for the CsCl and tetragonally distorted CsCl structures, and the (8,8,8) mesh for the rocksalt structure. This amounts to 10 points in the irreducible wedge of the Brillouin zone for the cubic structures, and to 18 in the case of tetragonal distortions. Plane waves up to a kinetic energy of 21 Ry were included in the basis set: This corresponds to ~ 1000 plane waves at equilibrium volume. The size of the basis set is varied accordingly to the volume of the unit cell. The crystal total energy is not yet fully converged even with such basis sets. The lack of total-energy convergence is a common feature in most calculations based on modern norm-conserving pseudopotentials which are relatively hard core. This is due to the difficulty to reproduce the details of the electronic wave functions inside the ionic core. These details are of course of little im-

TABLE I. Ionic pseudopotential parameters (a.u.) [see Eq. (2)].

Cesium $Z_v=9.00$, $\alpha_c=0.82$				
		$n=1$	$n=2$	$n=3$
$L=0$	α_n	3.22	3.48	3.81
	a_n	$4.870\,022\,085\,760\,76 \times 10^6$	$-1.669\,210\,385\,040\,69 \times 10^6$	$-3.200\,798\,779\,974\,08 \times 10^6$
	b_n	$-4.181\,401\,434\,279\,21 \times 10^5$	$-1.545\,101\,628\,782\,91 \times 10^6$	$-3.592\,271\,879\,200\,27 \times 10^5$
$L=1$	α_n	2.79	3.17	3.40
	a_n	$8.383\,238\,496\,285\,84 \times 10^5$	$3.500\,284\,280\,557\,49 \times 10^6$	$-4.338\,598\,376\,653\,02 \times 10^6$
	b_n	$-9.004\,204\,575\,933\,08 \times 10^4$	$-8.412\,265\,805\,919\,15 \times 10^5$	$-3.851\,879\,270\,042\,50 \times 10^5$
$L=2$	α_n	1.06	1.17	1.28
	a_n	$-1.028\,256\,417\,203\,60 \times 10^5$	$-4.824\,454\,833\,933\,24 \times 10^4$	$1.510\,725\,064\,292\,27 \times 10^5$
	b_n	$3.408\,227\,742\,193\,31 \times 10^3$	$1.844\,813\,873\,698\,44 \times 10^4$	$6.074\,843\,265\,486\,40 \times 10^3$
$L=3$	α_n	1.62	1.85	2.18
	a_n	$-1.616\,061\,743\,443\,15 \times 10^5$	$6.718\,907\,397\,219\,62 \times 10^4$	$9.439\,448\,941\,926\,05 \times 10^4$
	b_n	$1.203\,699\,710\,308\,82 \times 10^4$	$4.516\,883\,410\,784\,51 \times 10^4$	$1.112\,621\,811\,757\,38 \times 10^4$
Iodine $Z_v=1.00$, $\alpha_c=0.80$				
		$n=1$	$n=2$	$n=3$
$L=0$	α_n	2.76	3.12	3.35
	a_n	$7.443\,858\,220\,912\,63 \times 10^5$	$2.421\,831\,465\,482\,39 \times 10^6$	$-3.166\,206\,089\,821\,78 \times 10^6$
	b_n	$-7.752\,440\,418\,587\,25 \times 10^4$	$-6.425\,533\,114\,864\,58 \times 10^5$	$-2.761\,261\,744\,901\,89 \times 10^5$
$L=1$	α_n	2.31	2.55	2.79
	a_n	$7.761\,305\,828\,162\,69 \times 10^5$	$2.366\,710\,855\,530\,28 \times 10^5$	$-1.012\,793\,106\,898\,77 \times 10^6$
	b_n	$-5.807\,244\,098\,416\,03 \times 10^4$	$-2.846\,189\,412\,090\,50 \times 10^5$	$-8.665\,138\,141\,768\,01 \times 10^4$
$L=2$	α_n	1.26	1.37	1.61
	a_n	$1.020\,816\,125\,477\,17 \times 10^5$	$-8.341\,562\,607\,537\,61 \times 10^4$	$-1.866\,352\,106\,344\,40 \times 10^4$
	b_n	$-3.964\,264\,310\,322\,43 \times 10^3$	$-1.024\,891\,734\,020\,48 \times 10^4$	$-1.494\,127\,671\,120\,75 \times 10^3$
$L=3$	α_n	1.61	1.72	1.89
	a_n	$-3.635\,845\,818\,647\,86 \times 10^6$	$2.164\,102\,772\,617\,84 \times 10^6$	$1.471\,727\,381\,020\,54 \times 10^6$
	b_n	$1.359\,516\,226\,374\,84 \times 10^5$	$4.303\,455\,078\,853\,59 \times 10^5$	$8.384\,848\,857\,038\,31 \times 10^4$

portance in determining the structural properties of the materials, and we have indeed verified that the structural data we have calculated (lattice constant, bulk modulus, etc.), are converged to all the figures quoted in our tables. No use of perturbation theory is made to diagonalize such large matrices: All the plane waves have been treated exactly using a variant of the Davidson's block-iterative algorithm.¹³

III. STRUCTURAL PROPERTIES OF CSI

Total energies for different values of the unit-cell volume have been fitted to the second-order Keane equation of state,¹⁴

$$\frac{P(V)}{B_0} = \frac{B'_0}{N^2} \left[\left(\frac{V}{V_0} \right)^{-N} - 1 \right] + \ln \left(\frac{V}{V_0} \right) \frac{B'_0 - N}{N}, \quad (3)$$

where V_0 is the equilibrium volume, B_0 the bulk modulus, B'_0 and B''_0 are the first and second derivatives of B_0 with respect to pressure at $V=V_0$, and $N=B'_0+B_0B''_0/B'_0$. In Fig. 1 the energy-versus-volume curve of CsI is compared to the data calculated assuming a rocksalt crystal structure. This figure shows that contrary to the predictions of the semiempirical model of Ref. 3, first-principles calculations based on the LDA are indeed able to correctly predict the equilibrium crystal structure of CsI. In Table II we report the calculated values of the equilibrium lattice parameter, bulk modulus, and its derivatives with respect to pressure. The comparison with the corresponding experimental data^{1(d),15} is quite satisfactory. The (110) projection of the charge-density map of CsI at zero pressure is displayed in Fig. 2. The strong ionicity of CsI is revealed by the spherically piling of the charge at the ionic sites, with virtually no charge in between. The ionic character of CsI is of course

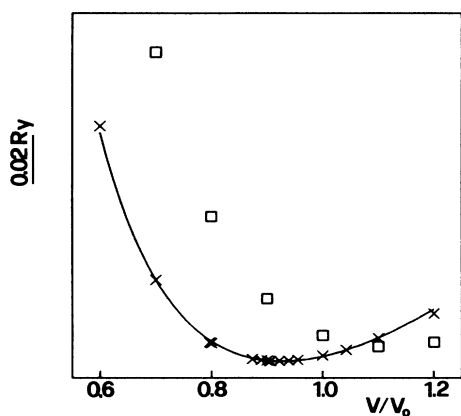


FIG. 1. Calculated crystal energy per cell of CsI as a function of the unit-cell volume (a.u.) referred to the observed zero-pressure volume V_0^* . Squares indicate data obtained assuming a CsI structure, crosses refer to the rocksalt structure. The continuous line is the result of a least-squares fit of the data to Eq. (3).

TABLE II. Lattice parameter a_0 , bulk modulus B_0 , and first two derivatives of B_0 with respect to pressure B'_0 and B''_0 , as calculated in this work for CsI and as given by experiments.

CsI	Present work	Asaumi ^a	Barsch and Chang ^b
a_0 (Å)	4.45	4.567	4.568
B_0 (kbar)	110	111±8	119±5
dB/dP	5.8	6.9±0.4	5.93±0.08
d^2B/dP^2	-0.07		

^aReference 1(d).

^bReference 15.

not surprising; however, former investigations based on the empirical pseudopotential scheme seemed to indicate a non-negligible covalency of the charge distribution of alkali halides.¹⁶ Only the recent availability of accurate first-principles calculations for such compounds¹⁷ finally clarified that the above covalency is an artifact due to the inaccuracy of the empirical pseudopotentials.

When CsI is squeezed at a volume of 0.54 of its equilibrium value, the cubic CsI phase becomes unstable and a tetragonal distortion spontaneously lowers the symmetry of the crystal.¹ In Fig. 3 we display the crystal energy per cell of CsI as a function of c/a (which has to be identified with the order parameter of the phase transition), for various values of the unit-cell volume. The transition volume is accurately reproduced by our calculation. Also the transition pressure, which according to Eq. (3) is 460 kbar, compares favorably with experiments. Figure 3 shows that the shear constant $c_s = (c_{11} - c_{12})/2$ (which is the elastic constant responsible for the stability of the cubic structure versus tetragonal distortions) decreases as the crystal is squeezed. The vanishing of c_s would signal a second-order transition. However at $V/V_0 \sim 0.54$, before the vanishing of c_s , a second minimum of E as a function of c/a appears at $c/a \sim 1.15$. According to our calculation, the transition is thus first order. This fact, although in agreement with other theoretical investigations and compatible with x-ray diffraction data which indicate an abrupt variation of c/a , seems to contradict optical ab-

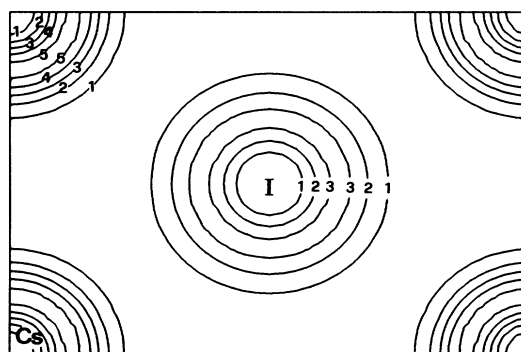


FIG. 2. Electron-charge-density distribution of CsI at equilibrium volume, projected onto the (110) plane. Units are 3×10^{-2} electrons per cubic Bohr radii.

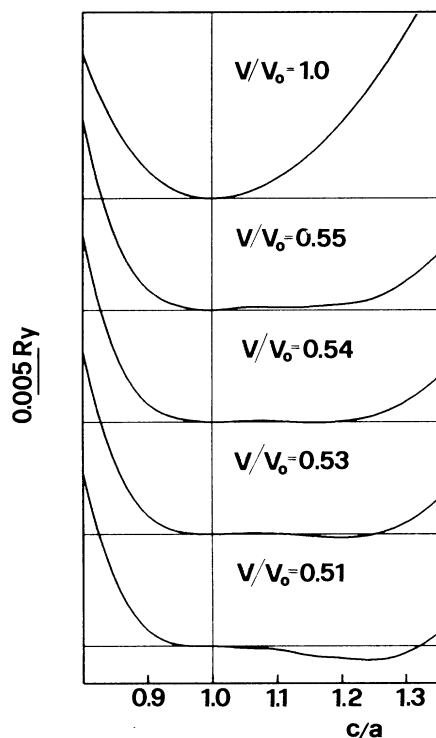


FIG. 3. Crystal energy per cell of CsI as a function of c/a for various volumes of the unit cell, referred to the calculated zero-pressure volume V_0 .

sorption measurements according to which the optical gap is continuous across the transition. In fact we calculated that, at $V/V_0=0.54$, the optical gap is lowered by ~ 0.3 eV as c/a is changed from 1 to its equilibrium value of 1.15. Although the LDA estimates of the optical gap are known to be unreliable,^{18,19} the qualitative dependence of E_g upon c/a is certainly within the predictive power of the LDA itself. We conclude that the results of optical experiments do not agree with structural data: The origin of this contradiction may lie in nonhydrostatic effects in the pressure distribution within the diamond cell. We cannot exclude the possibility of some inaccuracy in the experimental data: We just recall here that the determination of the metallization pressure of CsI is still a source of controversy.^{20–22}

In Fig. 4 we show the electron-charge-density distribution of CsI at $V/V_0=0.51$, both in the undistorted and in the distorted geometries. A superposition of Figs. 2 and 4(a) would bring out the following features: (i) the ionic charges stay almost unchanged during the compression; (ii) a slight isotropic compression of the ions is observed which results in more pronounced maxima in the pseudo-charges for the compressed geometry; (iii) the above effect is less pronounced for the cation than for the anion, as expected from the larger compressibility of the latter; (iv) the low-density levels at the frontier between the ionic and the interstitial regions differ considerably in the two figures, indicating an increasing hybridization between the anionic and cationic orbitals. This behavior is intimately

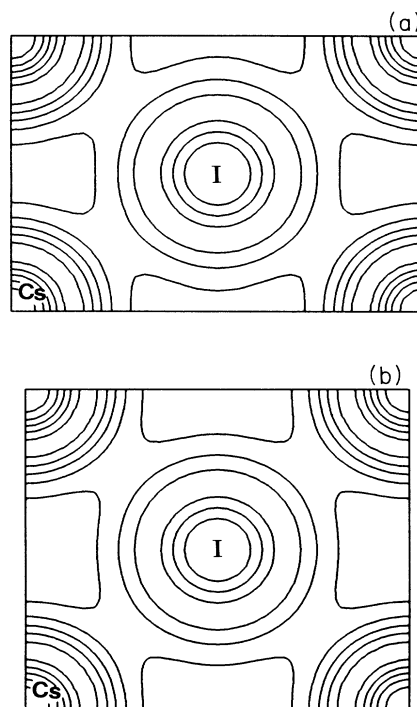


FIG. 4. Electron-charge-density distribution of CsI, at $V/V_0=0.51$, projected onto the (110) plane. (a) $c/a=1$; (b) $c/a=1.25$. Units and scale are the same as in Fig. 2.

related to the proximity of a band-overlap insulator-to-metal transition.

To clarify the mechanism of the structural transition, we define the crystal repulsive energy as the difference between the total-energy and the classical electrostatic (Madelung) interaction. The nature of this repulsive interaction is well illustrated by a comparison of Figs. 2 and 4, which indicates that the ionic sizes depend only very slightly on the interionic distance and that the ions behave therefore as (almost) hard spheres. Although the various contribution to the repulsive energy so defined have different physical origins (orthogonalization-induced interionic repulsion, short-range deviation from the point-like Madelung attraction, etc.), this definition allows a direct comparison with the semiempirical Born-Mayer model and suggests a pictorial description of the transition. In Fig. 5 we display, for CsI, both the Madelung and the negative of the repulsive energy for various volumes as a function of c/a , referred to their values at $c/a=1$. We notice that, at constant volume, the nearest-neighbor distance increases as c/a moves from 1. As a consequence, the attractive Madelung interaction stabilizes the cubic structure, while the repulsive one favors the tetragonal distortion. At low pressure, the electrostatic contribution to the total energy is far larger than the repulsive one, and the cubic phase is thus the most stable. As the volume decreases, the relative importance of the repulsive interaction increases, and, near the transition, the variations in the two contributions to the total energy

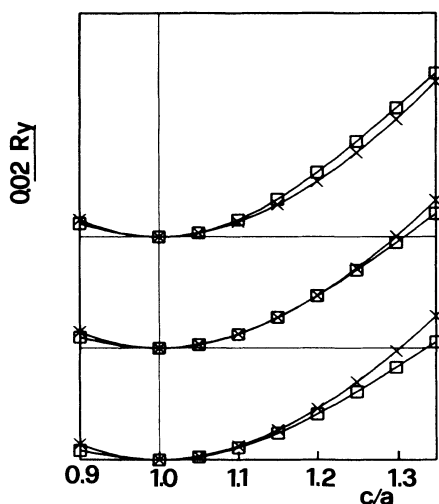


FIG. 5. Madelung energy (crosses) and negative of the repulsive energy (squares) as functions of c/a for CsI, for volumes close to the transition one. V_0 indicates the zero-pressure volume.

are of the same order. Just below the transition, the gain in the repulsive interaction with respect to Madelung energy favors the tetragonal distortion at $c/a > 1$, while the distortion for $c/a < 1$ is still unfavorable. This different behavior for c/a less than or greater than 1 signals the presence and the importance of a third-order term in the expansion of the energy as a function of $(c/a - 1)$, consistently with our conclusion that the transition is first order.

A second phase transition at a pressure of ~ 650 kbar has been reported in Refs. 1(d) and 1(f): On the basis of the splittings of the Bragg peaks in x-ray diffraction experiments, an isovolumic transition to an orthorhombic structure seems to take place. We have searched for such a transition varying the value of b/a and keeping the values of V fixed at $V/V_0 = 0.50$ and $c/a = 1.25$, but no transition has been found. As the paucity of experimental data does not allow a sure and unique determination of the distorted structure, we have tried a more complicated monoclinic distortion by allowing the angle between the a and c axis to vary, keeping the volume constant and $b = a$. Again, no evidence of a further transition has been found. Previous calculations based on the semiempirical Born-Mayer model were not able to predict such a transition,³ and no mention of it has been made in Ref. 5 where the cubic-to-tetragonal transition was successfully predicted by an *ab initio* LMTO calculation. Since not all the experimental investigations agree in the report of this further transition,¹ we conclude that further experimental and theoretical work is needed to elucidate its nature.

ACKNOWLEDGMENTS

S. B. wishes to thank Professor P. Erdős for the kind hospitality extended to him during a stay at the Institut de Physique Théorique of the University of Lausanne. P. G. is grateful to Professor M. Tosi for the hospitality offered to him by the International Centre for Theoretical Physics in Trieste. This work has been partially supported by the Swiss National Science Foundation, under Grant No. 2.683-085.

- ¹(a) E. Knittle and R. Jeanloz, *Science* **223**, 53 (1984); (b) J. Phys. Chem. Solids **46**, 1179 (1985); (c) T. L. Huang and A. L. Ruoff, *Phys. Rev. B* **29**, 1112 (1984); (d) K. Asaumi, *ibid.* **29**, 1118 (1984); (e) T. L. Huang, K. E. Brister, and A. L. Ruoff, *ibid.* **30**, 2968 (1984); (f) Y. K. Vohra, S. T. Weir, K. E. Brister, and A. L. Ruoff, *Phys. Rev. Lett.* **55**, 977 (1985).
²S. T. Weir, Y. K. Vohra, and A. L. Ruoff, *Phys. Rev. B* **33**, 4221 (1986).
³Y. K. Vohra, S. J. Duclos, and A. L. Ruoff, *Phys. Rev. Lett.* **54**, 570 (1985).
⁴P. Giannozzi (unpublished).
⁵N. E. Christensen and S. Satpathy, *Phys. Rev. Lett.* **55**, 600 (1985); S. Satpathy, N. E. Christensen, and O. Jepsen, *Phys. Rev. B* **32**, 6793 (1985).
⁶G. B. Bachelet and N. E. Christensen, *Phys. Rev. B* **31**, 879 (1985).
⁷D. R. Hamann, M. Schlueter, and C. Chiang, *Phys. Rev. Lett.* **43**, 1494 (1979).
⁸D. M. Ceperley and B. J. Alder, *Phys. Rev. Lett.* **45**, 566 (1980).
⁹J. Perdew and A. Zunger, *Phys. Rev. B* **23**, 5048 (1981).
¹⁰G. P. Kerker, *J. Phys. C* **13**, L189 (1980).
¹¹G. B. Bachelet, D. R. Hamann, and M. Schlueter, *Phys. Rev.*

- B* **26**, 4199 (1982).
¹²H. J. Monkhorst and J. P. Pack, *Phys. Rev. B* **13**, 5188 (1976).
¹³E. Davidson, in *Methods in Computational Molecular Physics*, edited by G. H. F. Diercksen and S. Wilson (Reidel, Dordrecht, 1983), p. 95.
¹⁴A. Keane, *Aust. J. Phys.* **7**, 322 (1954).
¹⁵G. R. Barsch and Z. P. Chang, *Natl. Bur. Stand. (U.S.) Publ. No. 326* (U.S. GPO, Washington, D.C., 1971), p. 173.
¹⁶S. Nagel, K. Maschke, and A. Baldereschi, *Phys. Status Solidi B* **76**, 1629 (1976).
¹⁷W. Andreoni, K. Maschke, and M. Schlueter, *Phys. Rev. B* **26**, 2314 (1982).
¹⁸W. Kohn, *Phys. Rev. B* **33**, 4331 (1986), and references quoted therein.
¹⁹Recent claims about the ability of LDA to predict the gap of CsI in the high-pressure regime [Refs. 5(b) and 20] (i.e., near metallization) seem to have been rebutted by accurate measurements of the metallization pressure (Refs. 21 and 22).
²⁰Y. K. Vohra, S. T. Weir, K. E. Brister, and A. L. Ruoff, *Phys. Rev. Lett.* **55**, 977 (1985).
²¹Q. Williams and R. Jeanloz, *Phys. Rev. Lett.* **56**, 163 (1986).
²²R. Reichlin, M. Ross, S. Martin, and K. A. Goettel, *Phys. Rev. Lett.* **56**, 2858 (1986).